CHEMISTRY
A EUROPEAN JOURNAL

ChemPubSoc
Europe

DOI: 10.1002/chem.201300064

Conformation and Atropisomeric Properties of Indometacin Derivatives

Shintaro Wakamatsu,[a] Yuka Takahashi,[a] Hidetsugu Tabata,[a] Tetsuta Oshitari,[a] Norihiko Tani,[a] Isao Azumaya,[b] Yukiteru Katsumoto,[c] Takeyuki Tanaka,[d] Shinzo Hosoi,[e] Hideaki Natsugari,[a] and Hideyo Takahashi*[a]

Abstract: The stereochemistry around the *N*-benzoylated indole moiety of indometacin was studied by restricting the rotation about the N−C7′ and/or C7′−C1′ bond. In the 2′,6′-disubstituted ones, an atropisomeric property was found and the atropoisomers were separated and isolated as stable forms. Their biological abilities to inhibit cyclooxygenase-1 (COX-1) and cyclooxygenase-2 (COX-2) were examined. Only the a*R*-isomer showed specific inhibition of COX-1, and COX-2 was not inhibited by either atropisomer. Conformational analysis in NMR studies and X-ray crystallography, and CD spectra in combination with calculations were utilized to elucidate the bioactive conformations.

Keywords: chirality · conformational analysis · drug design · nitrogen heterocycles · stereochemistry

Introduction

Indometacin is one of the most well-known non-steroidal anti-inflammatory drugs (NSAIDs). Its clinical use involves difficulty because it inhibits two isoforms of cyclooxygenase (COX-1 and COX-2) with little specificity, leading to serious side effects such as gastrointestinal bleeding and ulceration.[1] Therefore COX-1/2 selective indometacin analogues have been explored with the expectation of the development of a new generation of NSAIDs.[2] For the design of new indometacin analogues, the bioactive conformations complexed with COX-1/2 gave useful information. In 1996, the group of Loll and Gravito proposed that indometacin interacts with COX-1 in two possible binding modes corresponding to the *trans* or *cis* form.[3] Independently, another group reported that indometacin adopts a *cis* conformation in the complex with COX-2 (Figure 1 a).[4]

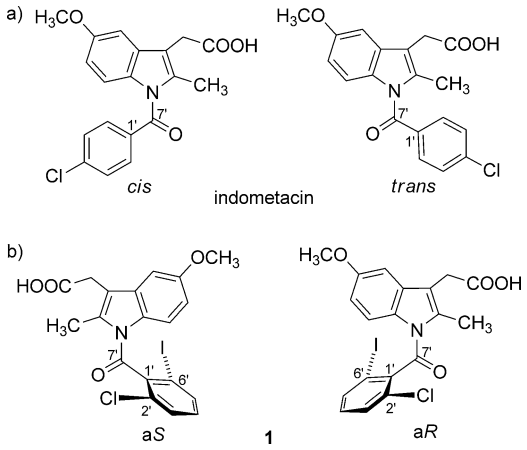

Figure 1. a) Conformations traditionally used for indometacin. b) 2′-Chloro-6′-iodo-substituted indometacin derivative **1**.

Since then, *trans/cis* conformations of indometacin have drawn much attention as key features for drug design.[5] However, a close look at the X-ray crystallographic analysis of indometacin revealed that the indole ring and benzoyl moiety are twisted with each other.[6] Therefore, the term "*cis*/*trans*" associated with images of the planar structure may cause misunderstanding. It should be realized that the *N*-benzoyl moiety has two sp^2–sp^2 axes (N−7′ bond and C7′−C1′ bond), which provide numerous conformations of indometacin. To elucidate the active conformation, restriction of the rotation about the N−C7′ bond and C7′−C1′ bond should be helpful. In the course of our study, we introduced substituents at C2′ and C6′ in benzoyl and succeeded in eliciting atropisomerism about the C7′−C1′ bond (Figure 1 b).[7] The isolation of each enantiomer of **1** (a*R*, a*S*) with high

[a] S. Wakamatsu, Y. Takahashi, Dr. H. Tabata, Dr. T. Oshitari, N. Tani, Prof. Dr. H. Natsugari, Prof. Dr. H. Takahashi
School of Pharmaceutical Sciences
Teikyo University, 2-11-1 Kaga
Itabashi-ku, Tokyo 173-8605 (Japan)
E-mail: hide-tak@pharm.teikyo-u.ac.jp

[b] Prof. Dr. I. Azumaya
Faculty of Pharmaceutical Sciences, Kagawa Campus
Tokushima Bunri University, 1314-1 Shido, Sanuki
Kagawa 769-2193 (Japan)

[c] Dr. Y. Katsumoto
Department of Chemistry, Graduate School of Science
Hiroshima University, Higashi-Hiroshima
Hiroshima 739-8256 (Japan)

[d] Dr. T. Tanaka
Integrated Center of Science, Ehime University, 3-5-7 Tarumi
Matsuyama, Ehime 790-8566 (Japan)

[e] Dr. S. Hosoi
Pharmaceutical Manufacturing Chemistry
Kyoto Pharmaceutical University, 1 Shichono-cho, Misasagi
Yamashina-ku, Kyoto 607-8412, (Japan)

Supporting information for this article is available on the WWW under http://dx.doi.org/10.1002/chem.201300064.

stereochemical stability confirmed that the rotation about the C7′–C1′ axis is fully restricted by substituents at C2′ and C6′, even though the N–C7′ axis can allow rotation. This atropisomerism serves as evidence of the rotational restriction of the C7′–C1′ axis. The interesting independent behavior of these two axes in solution led us to investigate further details of the rotational restriction about the two axes allowing isolation of the stable conformation. In this study, adding a significant data to the precedent one, we evaluated whether the substituents at the 2-position of the indole moiety and 2′- and/or 6′-position of the benzoyl moiety may restrict rotation about the N–C7′ and C7′–C1′ axes due to steric or electronic effects. We discuss the conformations of these indometacin analogues utilizing ^{1}H NMR spectroscopy, X-ray crystallography, and circular dichroism (CD) in combination with calculations.

Results and Discussion

First, we investigated the conformation of *N*-benzoylindoles in solution (Figure 2). Indometacin and related compounds

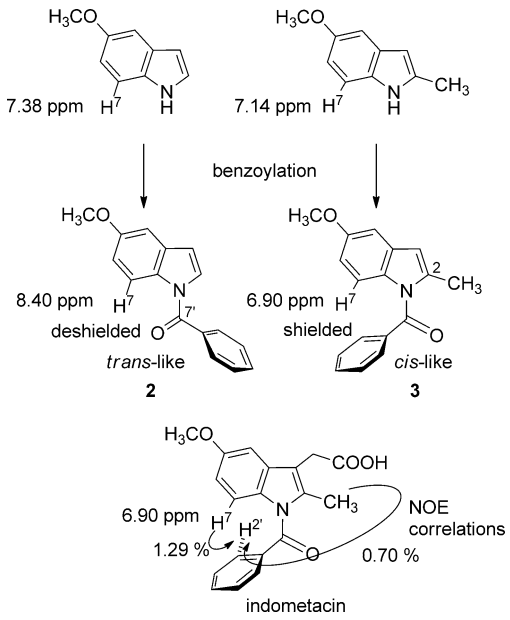

Figure 2. Conformational analysis based on the ^{1}H NMR spectra of indometacin and its analogues **2** and **3**.

(**2**,[8] **3**[9]) were characterized by using ^{1}H NMR spectroscopy with $CDCl_3$ as a solvent, which showed the characteristic resonances for H7 of indole units.

Whereas H7 in 5-methoxyindole (the mother compound of **2**) is observed at $\delta = 7.38$ ppm, H7 in **2** is observed at $\delta =$ 8.40 ppm. This downfield shift is caused by a deshielding effect of the carbonyl group of the benzoyl moiety, meaning that the benzoyl ring adopts a *trans*-like conformation with respect to the indole. In the case of 5-methoxy-2-methylindole (the mother compound of **3**), H7 is observed at $\delta =$ 7.14 ppm. Meanwhile, H7 of **3** is observed at $\delta = 6.90$ ppm. This upfield shift is due to the shielding effect of the benzene ring, meaning that the benzoyl ring adopts a *cis*-like conformation with respect to the indole (Figure 2). The opposite H7-shift observed in **2** and **3** indicates that *N*-benzoylated indole without a 2-methyl group adopts an intrinsically *trans*-like conformation and that the 2-methyl-substituted *N*-benzoylated indole adopts a *cis*-like conformation (Figure 2). It is obvious that steric hindrance caused by the substituent at the 2-position of indole mainly affects the N–C7′ axis, which regulates the *cis/trans*-like conformation. In indometacin, a 2-methyl-substituted *N*-benzoylated indole derivative, H7 is observed at $\delta = 6.90$ ppm, and thus its conformation should be *cis*-like, similar to **3**. In addition, NOE of indometacin seen between H7 and H2′ (1.29 %) and between 2-CH_3 and H2′ (0.70 %) indicates that its conformation is a rather *cis*-like one. We may therefore conclude that the characteristic resonance of H7 of the indole unit gives good information on the *cis/trans*-like conformation regulated by the N–C7′ axis of *N*-benzoylated indole derivatives.

We next examined the steric or electronic effects of the substituents at the 2-position of the indole and/or C2′ and C6′ of the benzoyl moiety. We synthesized various indometacin derivatives **4**–**6** and presumed their conformations mainly based on the H7-shift mentioned above (Table 1, Scheme 1).[10]

Table 1. H7 chemical shifts[a] of indometacin analogues **4**–**6**.

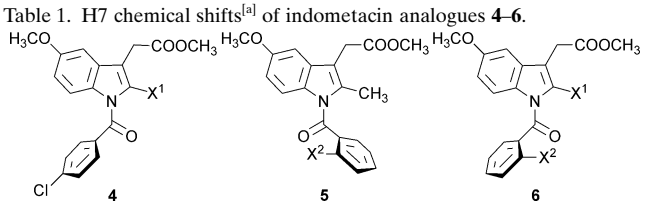

4	X^1	δ [ppm]	**5**	X^2	δ [ppm]	**6**	X^1	X^2	δ [ppm]
a	CH_3[b]	6.90	**a**	CH_3	6.96	**a**	CH_2Cl	Cl	6.45
b	CH_2Cl	6.57	**b**	CF_3	7.02	**b**	CH_2OH	Cl	6.05
c	CH_2OH	6.43	**c**	Cl	7.19	**c**	CH_2Cl	I	6.45
d	CH_2OTBS	6.77	**d**	Br	7.21	**d**	CH_2OH	I	5.91
e	CHO	7.37	**e**	I	7.14	**e**	CHO	I	6.99

[a] Recorded at 23 °C in $CDCl_3$ with TMS as internal reference. [b] Indometacin methyl ester.

For all of these compounds, only one set of resonances (*cis*- or *trans*-like) was observed in the ^{1}H NMR spectrum.[11] In compounds **4a**–**d**, H7 is observed at $\delta = 6.43$–6.90 ppm, which confirms that the compounds with bulkier substitutes at C2 adopt a *cis*-like conformation as mentioned above. On the other hand, in compounds **5a**–**e**, H7 is observed at $\delta =$ 6.96–7.21 ppm. Such a downfield shift supports that the compounds with substitutes at C2′ of the benzoyl group adopt a *trans*-like conformation.[12] It was found that substitution at the C2′ position of the benzoyl group also affects the rotation of the N–C7′ axis. In compounds **6a**–**d**, H7 is observed at $\delta = 5.91$–6.45 ppm, which confirms that the compounds with bulkier substitutes at both C2 and C2′ adopt a *cis*-like

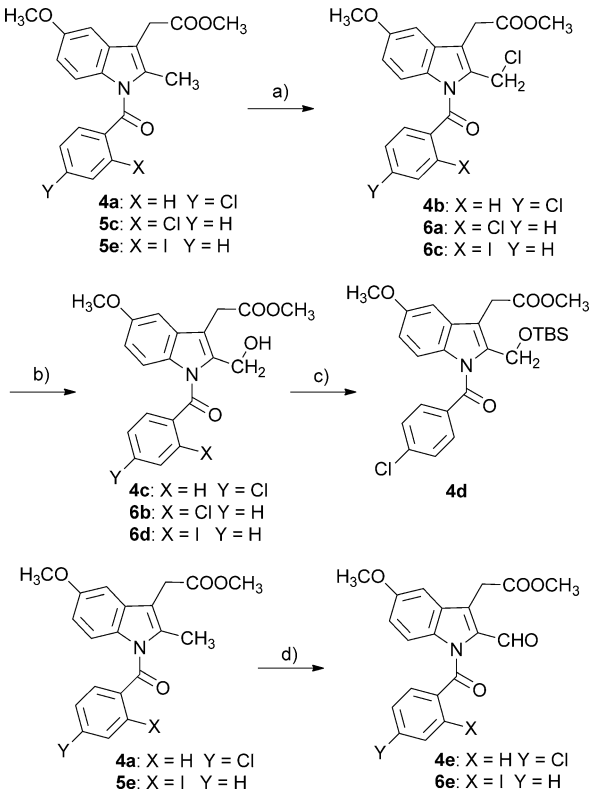

Scheme 1. Synthesis of indometacin derivatives **4**–**6**: a) NCS, BPO, CCl_4, heat at reflux, 2.5 h, 70% for **4b**, 70% for **6a**, 81% for **6c**; b) $AgNO_3$, THF/H_2O, RT, 25 min, 64% for **4c**, 66% for **6b**, 42% for **6d**; c) TBSOTf, 2,6-lutidine, CH_2Cl_2, 0°C, 10 min, 78%; d) NCS, BPO, CCl_4, heat at reflux, 5 h, 63% for **4e**, 13% for **6e**.

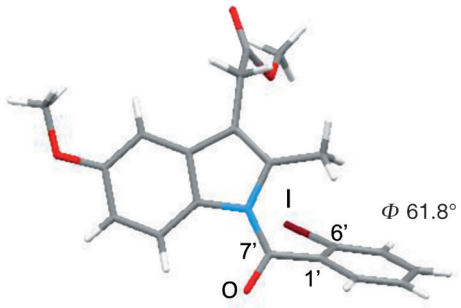

Figure 3. Structure of **5e** determined by using X-ray crystallographic analysis.

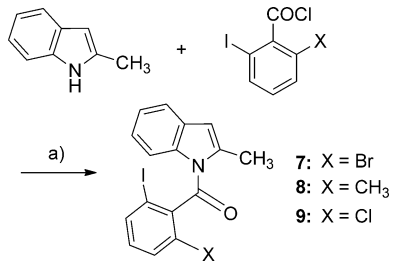

Scheme 2. Synthesis of derivatives **7**–**9**: a) KHMDS, ArCOCl, THF, RT, 2 h, 22% for **7**, 28% for **8**, 45% for **9**.

conformation. It is interesting that a different downfield shift was observed in **4e** and **6e** with a formyl group at C2. The apparent *trans*-like conformation is due to carbonyl electronic repulsion of the benzoyl group away from the formyl group at C2. It seems reasonable to assume that the *cis*- or *trans*-like conformation of indometacin and related compounds **2**–**6** mentioned above is typical in solution and the H7 shift may provide a clue to determining the rotation of the N−C7′ axis.

We next examined the C7′−C1′ axis in indometacin derivatives. Unfortunately, separation analysis of compounds **2**–**6** by using chiral HPLC provides only one peak at room temperature, which means that the atropisomeric property arising from the C7′−C1′ axis does not exist in these compounds. However, the single-crystal X-ray analysis of compound **5e** gave meaningful information. The dihedral angle (Φ) C6′−C1′−C7′−O of 61.8° in compound **5e** confirmed that the benzene ring is orthogonal to the indole ring (Figure 3). This geometry convinced us that even a monosubstituent at C2′ of benzoyl can essentially affect the rotation of the C7′−C1′ axis, although the rotational barrier is less than required for the isolation of each enantiomer.

We therefore focused on the C2′- and C6′-disubstituted derivatives **7**–**9**, which were synthesized as shown in Scheme 2. In all of these compounds, as well as in **1**, two sets of resonances corresponding to *cis*- and *trans*-like conformations are observed in the ^{1}H NMR spectrum (*cis*-like/*trans*-like = 1:1.4–2.0). We assigned the *cis*/*trans* comformations using a combination of the H7 shift as mentioned above and the NOESY spectrum of **1** reported in a previous paper.[7] Because the rotational barrier of the N−C7′ axis is less than that required for the isolation of each conformer at room temperature, compounds **7**–**9** were observed as one peak on non-chiral HPLC at ambient temperature. However, each was observed as two separate peaks when analyzed in HPLC on a chiral column (CHIRALPAK IB) at room temperature, indicating that they exist as racemates of the atropisomers. It is clear that steric hindrance caused by substituents at C2′ and C6′ forms a greater rotational barrier to the C7′−C1′ axis than to the N−C7′ axis. It should be noted that each *cis*- and *trans*-like conformation of *N*-benzoylated indole derivatives **7**–**9** exists as racemates of the a*R* and a*S* isomers (Figure 4).

The enantiomers of compounds **7**–**9** were successfully isolated by using preparative chiral HPLC (CHIRALPAK IB). The isolated atropisomers have opposite $[\alpha]_D$ values: **7A** (with shorter retention time in HPLC) as 96.4% *ee* showed $[\alpha]_D^{20} = -32.5$ ($c = 0.2$, $CHCl_3$) and **7B** (with longer retention time in HPLC) as 98.5% *ee* showed $[\alpha]_D^{20} = +31.7$ ($c = 0.2$, $CHCl_3$), **8A** (with shorter retention time in HPLC) as 98.8% *ee* showed $[\alpha]_D^{20} = -28.6$ ($c = 0.2$, $CHCl_3$) and **8B** (with longer retention time in HPLC) as 95.8% *ee* showed $[\alpha]_D^{20} = +24.6$ ($c = 0.2$, $CHCl_3$), and **9A** (with shorter retention time in HPLC) as 99.9% *ee* showed $[\alpha]_D^{20} = -26.1$ ($c = 0.2$, $CHCl_3$) and **9B** (with longer retention time in HPLC)

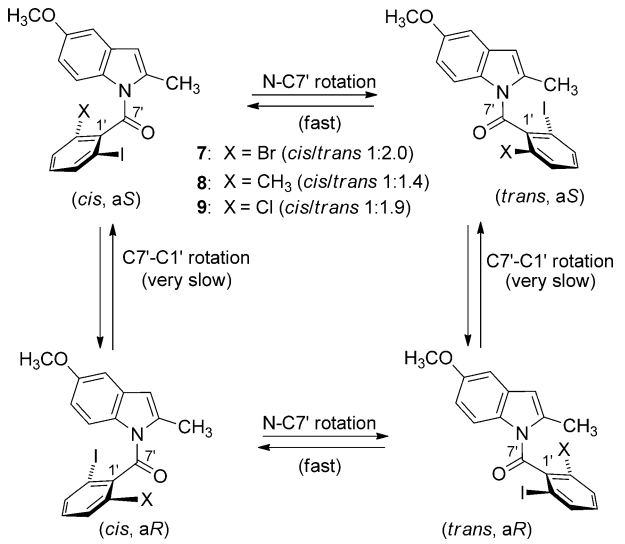

Figure 4. Conformers including atropisomers of the *N*-benzoylated indole derivatives **7**–**9**.

as 99.9% *ee* showed $[\alpha]_D^{20} = +18.8$ ($c = 0.2$, $CHCl_3$). We also examined the stereochemical stability of the enantiomers and found that it was estimated to be high. The higher stereochemical stability with a $\Delta G^{\ddagger}$ value[13] of 109 kJ mol^{-1} for **8A** and **8B** (X = CH_3), and 111 kJ mol^{-1} for **7A** and **7B** (X = Br), compared with 105 kJ mol^{-1} for **9A** and **9B** (X = Cl) may be explained largely because of the steric bulkiness (van der Waals radius) of the methyl (2.0 Å) and Br (1.85 Å) versus Cl (1.75 Å). Also, some type of electronic effect may affect the rotational barrier of the C7′–C1′ axis by controlling the electronic density on the benzene ring.

We next examined the relationship with axial chirality and biological activity. The racemate of **1** or its enantiomers did not show COX-2 inhibitory activity at a concentration of 500 μM. However, it was found that the (+)-enantiomer of **1** shows potent activity against COX-1 with an IC_{50} value of (15.6 ± 1.8) μM. The other (−)-enantiomer showed no inhibitory activity at a concentration of 200 μM (Table 2).[7,14]

Table 2. In vitro cyclooxygenase assay of **1** (racemate and atropisomers).

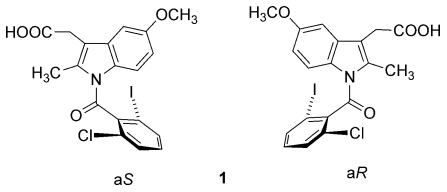

	$[\alpha]_D^{22}$ ($CHCl_3$)	IC_{50} [μM] COX-1	COX-2
1 (racemate)		13.4 ± 3.4	> 500
(−)-**1**	−21.2 (c = 0.13, 96% *ee*)	> 200	> 500
(+)-**1**	+20.4 (c = 0.10, 94% *ee*)	15.6 ± 1.8	> 500
indometacin		0.106 ± 0.042	3.50 ± 0.41

The results clearly indicate that COX-1 recognizes the stereochemistry of the axial chirality arising from the C7′–C1′ axis. Initially, efforts to obtain the absolute configuration of these atropisomers by X-ray crystallography were not successful. Therefore the stereochemical information on them was obtained by circular dichroism (CD) in combination with calculations.

A conformational search by using molecular mechanical calculation (CONFLEX-MMFF94s) in vacuo for *cis/trans* conformers yielded 32 conformers for each enantiomer (a*S*-**1**, a*R*-**1**). All conformers were then fully optimized by using DFT at the B3LYP/6-31G(d) level with the LANL2DZ basis sets for iodine, affording only eight conformers [*cis*-a*S*-**1** (1), *cis*-a*S*-**1** (2), *cis*-a*R*-**1** (1), *cis*-a*R*-**1** (2), *trans*-a*S*-**1** (1), *trans*-a*S*-**1** (2), *trans*-a*R*-**1** (1), *trans*-a*R*-**1** (2)] lying in a range of 2 kJ mol^{-1} (Figure 5). Based on those real energy minima (no imaginary frequencies) for these conformers, the energy values with the zero-point energy correction were calculated. The relative energies and their conformational distributions are given in Table 3.

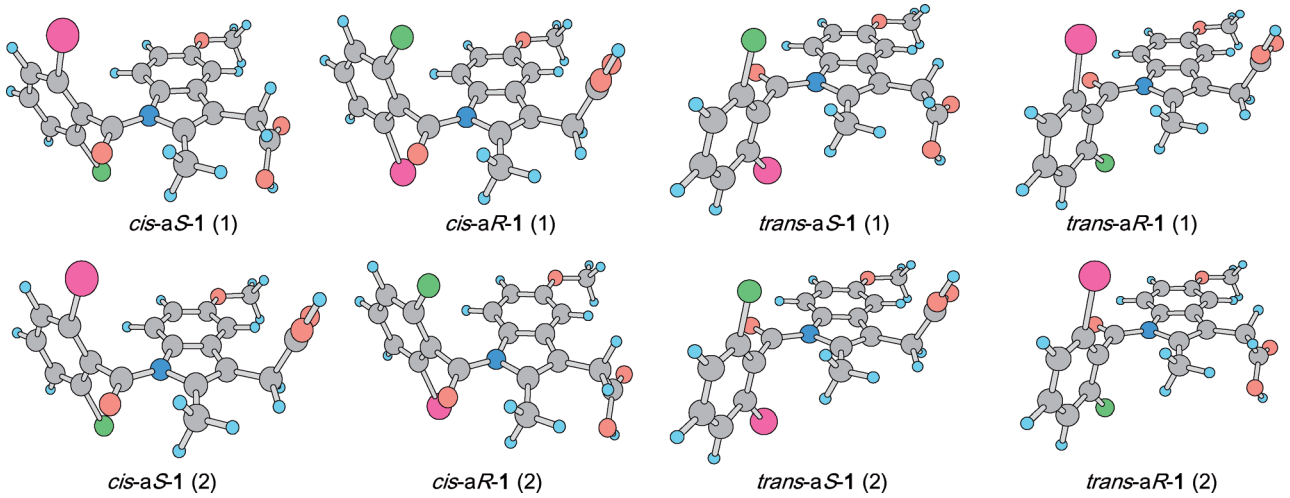

Figure 5. Low-energy conformers of a*S*-**1** and a*R*-**1**, as was calculated by DFT methods.

Table 3. Conformational analysis of **1**.

Conformer	ΔE [kJ mol^{-1}]	Boltzmann factor
cis-a*S*-**1** (1)	0.000	1.000
cis-a*R*-**1** (1)	0.000	1.000
cis-a*S*-**1** (2)	0.07879	0.9687
cis-a*R*-**1** (2)	0.07879	0.9687
trans-a*S*-**1** (1)	1.397	0.5752
trans-a*R*-**1** (1)	1.371	0.5691
trans-a*S*-**1** (2)	1.613	0.5352
trans-a*R*-**1** (2)	1.550	0.5218

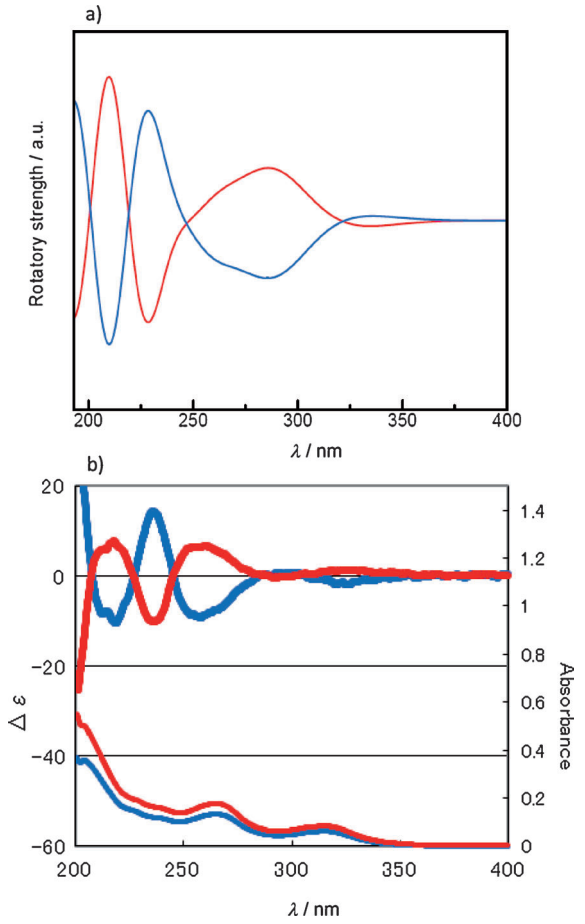

Figure 6. a) Calculated CD spectra of a*R*-**1** (red, averaged) and a*S*-**1** (blue, averaged). b) Experimental UV and CD spectra of (+)-**1** (red) and (−)-**1** (blue).

The CD calculations for the conformers were then conducted with the same level of calculation. The calculated CD spectra, weighted based on the Boltzmann factor of both a*S* and a*R* enantiomers, are shown in Figure 6, along with the experimental CD of (−)-**1** and (+)-**1** in EtOH, which were symmetrical to the *x* axis for the antipodal pairs, indicating that the two isomers are enantiomeric to each other in solution. The weighted CD spectra for the a*S*/a*R* enantiomer of **1** are in good accordance with the experimental ones for (−)/(+)-**1**, respectively. Therefore, we presumed that (−)-**1** can be assigned as a*S* and (+)-**1** as a*R*.

After some time, we fortunately succeeded in obtaining (−)-**1** as a single crystal.[7] On the basis of X-ray analysis,[7] (−)-**1** was also assigned to be a*S*, and hence the bioactive atropisomer (+)-**1** is a*R*. It should be noted that the assignments of the configurations of **1** based on the calculated CD spectra agree with those obtained by using X-ray analysis. However, the calculated *cis* preferential formation shown in Table 3 differed from the *trans* preferential one confirmed by ^{1}H NMR spectra, resulting in an underestimation of the importance of the *cis*/*trans* ratio in the geometric optimization of **1**. Furthermore, conformational analysis using X-ray crystallography showed that (−)-**1** crystallized only in the *cis* form (Figure 7), which was not identical to the results in the ^{1}H NMR analysis. Although this discrepancy needs further consideration, it seems reasonable to say that the twisted conformation including atropisomerism arising from the C7′–C1′ axis in **1** might hamper the binding to COX-2 (Table 2). We presume that the restriction of the rotation about the C7′–C1′ axis instead of the N–C7′ axis might be informative for the design of COX-1/2-selective drugs.

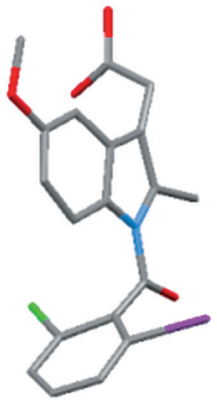

Figure 7. Structure of (−)-**1** determined by using X-ray crystallographic analysis.[7]

Conclusion

The introduction of substituents at the 2-position of the indole moiety and 2′- and/or the 6′-position of the benzoyl moiety succeeded in eliciting specific conformations through the restriction of the rotation about the N–C7′ axis and C7′–C1′ axis. The characteristic resonance for H7 of the indole unit in ^{1}H NMR spectra serves as a clue to the *cis*/*trans*-like formation of indometacin derivatives. It was also revealed that atropisomers of 2′,6′-disubstituted derivatives exist with high stereochemical stability and can be separated and isolated by chiral HPLC. It is noteworthy that this new chirality occurs by fixing of the C7′–C1′ axis alone, and hence, the other N–C7′ axis independently rotates to form an equilibrium between *cis*- and *trans*-like conformations in each enantiomer. For the determination of the configuration of the bioactive atropisomer (+)-**1**, the calculated CD spectrum, which is in good accordance with the experimental one, was strongly supportive of the structure determined by X-ray crystallographic analysis. The atropisomeric property arising from the C7′–C1′ axis may be useful in the development of next-generation NSAIDs.

Experimental Section

General experimental procedures: All reactions sensitive to air or moisture were conducted under an argon atmosphere. Materials were obtained from commercial suppliers. All anhydrous solvents were purified following standard methods. Melting points were determined on a Yanagimoto micro melting point apparatus and were uncorrected. The NMR spectra (^{1}H, ^{13}C) were determined on a JEOL 600 MHz (ECP-600) or 400 MHz (AL-400) spectrometer at 23 °C, using $CDCl_3$ (with TMS for ^{1}H NMR spectroscopy and $CDCl_3$ for ^{13}C NMR spectroscopy as the internal reference) solution, unless otherwise noted. Chemical shifts are given in parts per million (ppm) downfield from tetramethylsilane as an internal standard, and coupling constants (J) are reported in Hertz (Hz). Splitting patterns are abbreviated as follows: singlet (s), doublet (d), and triplet (t). High-resolution mass spectra (HRMS) were obtained on LCMS-IT-TOF (Shimadzu, Kyoto, Japan) for electrospray ionization (ESI). Sodium trifluoroacetate (TFA-Na) was used as an internal standard for HRMS. Optical rotations were determined using a DIP-370 (Shimadzu, Kyoto, Japan) digital polarimeter in 100 mm cells and the sodium D line (589 nm) at room temperature in the solvent and at the concentration indicated. Infrared (IR) spectra were recorded on a JASCO FT/IR-410 spectrometer by using sodium chloride plates or potassium bromide pellets. Absorbance frequencies were recorded in reciprocal centimeters (cm^{-1}). CD and UV spectra were recorded on a JASCO J-725. Analytical thin-layer chromatography was carried out using Merck silica gel 60 F_{254}. Column chromatography was performed by using the silica gel Wakogel C-300 (45–60 μm).

Compound 4b, methyl [1-(4-chlorobenzoyl)-2-chloromethyl-5-methoxy-1*H*-indol-3-yl]acetate: Benzoyl peroxide (BPO; 4.8 mg, 0.02 mmol) was added to a solution of **4a** (79 mg, 0.21 mmol) and NCS (56 mg, 0.42 mmol) in CCl_4 (5 mL). After stirring for 2.5 h and heating at reflux, the reaction was quenched with H_2O and extracted with CH_2Cl_2. The organic layer was dried over Na_2SO_4. After evaporation in vacuo, the crude residue was purified by silica gel column chromatography (Et_2O/hexane, 1:1) to give **4b** (60 mg, 0.15 mmol, 70%) as a colorless oil. Analytical data: ^{1}H NMR (400 MHz, $CDCl_3$): δ = 3.73 (3H, s), 3.79 (2H, s), 3.84 (3H, s), 5.08 (2H, s), 6.57 (1H, d, J = 8.8 Hz), 6.71 (1H, dd, J = 2.4 Hz, 8.8 Hz), 7.02 (1H, d, J = 2.4 Hz), 7.49 (2H, d, J = 8.4 Hz), 7.72 (2H, d, J = 8.4 Hz); ^{13}C NMR (100 MHz, $CDCl_3$): δ30.1, 35.6, 52.1, 55.7, 101.2, 111.5, 112.4, 114.8, 129.0, 129.2, 130.5, 131.0, 131.3, 133.8, 135.8, 139.1, 155.9, 168.1, 171.2 ppm; IR (neat): $\tilde{\nu}$ = 1738, 1684 cm^{-1}; HRMS (ESI): m/z calcd for $C_{20}H_{17}NO_4Cl_2$ Na: 428.0427 [M+Na]; found: 428.0406.

Compound 4c, methyl [1-(4-chlorobenzoyl)-2-hydroxymethyl-5-methoxy-1*H*-indol-3-yl]acetate: A solution of $AgNO_3$ (10.0 mg, 0.056 mmol) in H_2O (1 mL) was added to a solution of **4b** (22.7 mg, 0.056 mmol) in THF/H_2O (2:1, 2 mL) and stirred at room temperature for 25 min. The reaction was diluted with H_2O and extracted with $CHCl_3$. The organic layer was washed with brine and dried over Na_2SO_4. After evaporation in vacuo, the crude residue was purified by silica gel column chromatography (EtOAc/hexane, 1:2) to give **4c** (13.8 mg, 0.036 mmol, 64%) as a colorless oil. ^{1}H NMR (400 MHz, $CDCl_3$): δ = 3.73 (3H, s), 3.82 (2H, s), 3.83 (3H, s), 3.93 (1H, brt, J = 7.2), 4.79 (2H, d, J = 7.2 Hz), 6.43 (1H, d, J = 9.2 Hz), 6.66 (1H, dd, J = 2.4, 9.2 Hz), 7.00 (1H, d, J = 2.4 Hz), 7.50 (2H, d, J = 8.8 Hz), 7.69 ppm (2H, d, J = 8.8 Hz); ^{13}C NMR (100 MHz, $CDCl_3$): δ = 30.0, 52.4, 55.0, 55.7, 102.0, 113.1, 115.2, 115.3, 128.3, 129.2, 130.0, 130.3, 130.6, 131.1, 133.0, 139.1, 139.6, 156.2, 168.9, 171.1 ppm; IR (neat): $\tilde{\nu}$ = 3503, 1736, 1672 cm^{-1}; HRMS (ESI) m/z calcd for $C_{20}H_{18}NO_5ClNa$ [M+Na]: 410.0766; found: 410.0773.

Compound 4d, methyl [2-*tert*-butyldimethylsiloxymethyl-1-(4-chlorobenzoyl)-5-methoxy-1*H*-indol-3-yl]acetate: TBSOTf (10.1 mg, 9 μL, 0.038 mmol) was added to a solution of **4c** (7.4 mg, 0.019 mmol) and 2,6-lutidine (4.5 mg, 5 μL, 0.042 mmol) in CH_2Cl_2 (1 mL) was added. After stirring for 10 min at 0 °C, the reaction was quenched with H_2O and extracted with CH_2Cl_2. The organic layer was washed with brine and dried over Na_2SO_4. After evaporation in vacuo, the crude residue was purified by silica gel column chromatography (EtOAc/hexane, 1:2) to give **4d** (7.5 mg, 0.015 mmol, 78%) as a colorless oil. ^{1}H NMR (400 MHz, $CDCl_3$): δ = −0.10 (6H, s), 0.71 (9H, s), 3.63 (3H, s), 3.73 (2H, s), 3.77 (3H, s), 4.82 (2H, s), 6.65 (1H, dd, J = 2.4, 9.0 Hz), 6.77 (1H, d, J = 9.0 Hz), 6.93 (1H, d, J = 2.4 Hz), 7.39 (2H, d, J = 8.3 Hz), 7.63 ppm (2H, d, J = 8.3 Hz); ^{13}C NMR (100 MHz, $CDCl_3$): δ = −5.5, 18.3, 25.8, 30.3, 52.2, 55.8, 56.5, 101.6, 112.8, 113.0, 114.6, 128.9, 129.9, 131.1, 131.4, 133.5, 138.0, 139.3, 155.7, 168.1, 171.1 ppm; IR (neat): $\tilde{\nu}$ = 1740, 1691 cm^{-1}; HRMS (ESI) m/z calcd for $C_{26}H_{32}NO_5SiCl$: 524.1636 [M+Na]; found: 524.1623.

Compound 4e, methyl [1-(4-chlorobenzoyl)-2-formyl-5-methoxy-1*H*-indol-3-yl]acetate: BPO (106.8 mg, 0.44 mmol) was added to a solution of **4a** (1.64 g, 4.41 mmol) and NCS (1.77 g, 13.2 mmol) in CCl_4 (30 mL). After stirring for 5 h heated at reflux, the reaction was quenched with H_2O and extracted with CH_2Cl_2. The organic layer was dried over Na_2SO_4. After evaporation in vacuo, the crude residue was purified by silica gel column chromatography (Et_2O/hexane, 1:2) to give **4e** (1.07 g, 2.77 mmol, 63%) as a white solid. M.p. 108 °C; ^{1}H NMR (400 MHz, $CDCl_3$): δ = 3.72 (3H, s), 3.85 (3H, s), 4.14 (2H, s), 7.05 (2H, m), 7.37 (1H, d, J = 9.0 Hz), 7.47 (2H, d, J = 8.6 Hz), 7.68 (2H, d, J = 8.6 Hz), 9.82 ppm (1H, s); ^{13}C NMR (100 MHz, $CDCl_3$): δ = 30.4, 52.7, 56.1, 102.3, 116.3, 119.7, 125.1, 129.7, 130.0, 131.7, 133.1, 133.9, 135.0, 140.8, 157.5, 168.1, 171.0, 182.7 ppm; IR (KBr): $\tilde{\nu}$ = 1740, 1684 cm^{-1}; HRMS (ESI) m/z calcd for $C_{20}H_{16}NO_5Cl$: 408.0609 [M+Na]; found: 408.0612.

Compound 6a, methyl [1-(2-chlorobenzoyl)-2-chloromethyl-5-methoxy-1*H*-indol-3-yl]acetate: BPO (15 mg, 0.01 mmol) was added to a solution of **5c** (211 mg, 0.57 mmol) and NCS (227 mg, 1.7 mmol) in CCl_4 (5 mL). After stirring for 2.5 h with heating at reflux, the reaction was quenched with H_2O and extracted with CH_2Cl_2. The organic layer was dried over Na_2SO_4. After evaporation in vacuo, the crude residue was purified by silica gel column chromatography (Et_2O/hexane, 1:1) to give **6a** (162 mg, 0.40 mmol, 70%) as a colorless oil. ^{1}H NMR (400 MHz, $CDCl_3$): δ = 3.65 (3H, s), 3.72 (2H, s), 3.75 (3H, s), 5.01 (2H, s), 6.45 (1H, d, J = 9.2 Hz), 6.61 (1H, dd, J = 2.4, 9.2 Hz), 6.93 (1H, d, J = 2.4 Hz), 7.42 ppm (4H, m); ^{13}C NMR (100 MHz, $CDCl_3$): δ = 29.8, 36.6, 52.4, 55.6, 102.0, 114.2, 114.6, 117.4, 127.2, 129.7, 129.9, 130.4, 130.6, 131.9, 132.3, 134.4, 135.1, 156.3, 165.8, 170.2; IR (neat): $\tilde{\nu}$ = 1740, 1694 cm^{-1}; HRMS (ESI) m/z calcd for $C_{20}H_{17}NO_4Cl_2$: 428.0432 [M+Na]; found: 428.0441.

Compound 6b, methyl [1-(2-chlorobenzoyl)-2-hydroxymethyl-5-methoxy-1*H*-indol-3-yl]acetate: A solution of $AgNO_3$ (5.0 mg, 0.03 mmol) in H_2O (1 mL) was added to a solution of **6a** (11 mg, 0.03 mmol) in THF/H_2O (2:1, 1 mL) and stirred at room temperature for 1 h. The reaction was diluted with H_2O and extracted with AcOEt. The organic layer was washed with brine and dried over Na_2SO_4. After evaporation in vacuo, the crude residue was purified by silica gel column chromatography (EtOAc/hexane, 1:1) to give **6b** (7.0 mg, 0.02 mmol, 66%) as a colorless oil. ^{1}H NMR (400 MHz, $CDCl_3$): δ = 3.67 (3H, s), 3.77 (5H, s), 4.87 (2H, s), 6.05 (1H, d, J = 9.2), 6.58 (1H, dd, J = 2.4, 9.2 Hz), 6.98 (1H, d, J = 2.4 Hz), 7.52 ppm (4H, m); ^{13}C NMR (100 MHz, $CDCl_3$): δ = 30.0, 52.4, 55.4, 55.6, 102.4, 113.3, 114.4, 116.2, 127.5, 129.1, 129.7, 130.5, 131.1, 131.6, 132.3, 135.4, 138.6, 156.4, 170.0, 170.8 ppm; IR (neat): $\tilde{\nu}$ = 3513, 2953, 1738, 1676 cm^{-1}; HRMS (ESI) m/z calcd for $C_{20}H_{18}NO_5Cl$: 410.0766 [M+Na]; found: 410.0771.

Compound 6c, methyl [2-chloromethyl-1-(2-iodobenzoyl)-5-methoxy-1*H*-indol-3-yl]acetate: Compound **5e** (27.1 mg, 0.059 mmol) was subjected to reaction with NCS (7.8 mg, 0.059 mmol) and BPO (1.4 mg, 0.0059 mmol) following the same procedure as that used for the synthesis of **6a** described above to afford the product **6c** (23.5 mg, 0.047 mmol, 81%) as a colorless oil. ^{1}H NMR (600 MHz, $CDCl_3$): δ = 3.72 (3H, s), 3.79 (2H, s), 3.82 (3H, s), 5.05 (2H, d, J = 3.6 Hz), 6.45 (1H, d, J = 9.0 Hz), 6.69 (1H, dd, J = 2.4, 9.0 Hz), 7.00 (1H, d, J = 2.4 Hz), 7.29 (1H, m), 7.50 (2H, m), 7.97 ppm (1H, d, J = 7.8 Hz); ^{13}C NMR (100 MHz, $CDCl_3$): δ = 30.7, 35.9, 52.4, 55.7, 102.0, 113.1, 114.3, 115.2, 128.6, 128.9, 130.0, 132.3, 132.6, 136.0, 156.3, 167.9, 170.8 ppm; IR (neat): $\tilde{\nu}$ = 1740, 1694 cm^{-1}; HRMS (ESI) m/z calcd for $C_{20}H_{17}NO_4ClI$: 519.9789 [M+Na]; found: 519.9776.

Compound 6d, methyl [2-hydroxymethyl-1-(2-iodobenzoyl)-5-methoxy-1*H*-indol-3-yl]acetate: Compound **6c** (19 mg, 0.038 mmol) was treated with $AgNO_3$ (6.4 mg, 0.038 mmol) following the same procedure as that used for the synthesis of **6b** described above to afford the product **6d** (7.5 mg, 0.016 mmol, 42%) as a colorless oil. ^{1}H NMR (400 MHz, $CDCl_3$): δ = 3.65 (3H, s), 3.74 (5H, s), 4.80 (2H, s), 5.91 (1H, d, J =

9.3 Hz), 6.51 (1H, dd, J=2.7, 9.3 Hz), 6.91 (1H, d, J=2.7 Hz), 7.24 (1H, t, J=7.6 Hz), 7.41 (1H, d, J=7.6 Hz), 7.48 (1H, t, J=7.6 Hz), 7.89 ppm (1H, d, J=7.6 Hz); ^{13}C NMR (100 MHz, $CDCl_3$): δ=30.0, 52.4, 55.5, 55.6, 92.7, 102.3, 113.3, 114.8, 116.3, 128.8, 128.9, 129.7, 131.2, 132.2, 138.8, 140.1, 141.3, 156.4, 169.1, 170.8 ppm; IR (neat): $\tilde{\nu}$=3507, 2951, 1736, 1672 cm^{-1}; HRMS (ESI) m/z calcd for $C_{20}H_{18}NO_5Ina$: 502.0122 [M+Na]; 502.0100.

Compound (6e), methyl [2-formyl-1-(2-iodobenzoyl)-5-methoxy-1*H*-indol-3-yl]acetate: BPO (6.5 mg, 0.027 mmol) was added to a solution of **5e** (124 mg, 0.27 mmol) and NCS (89.4 mg, 0.67 mmol) in CCl_4 (8 mL) was added. After stirring for 5 h while heating at reflux, the reaction was quenched with H_2O and extracted with CH_2Cl_2. The organic layer was dried over Na_2SO_4. After evaporation in vacuo, the crude residue was purified by silica gel column chromatography (EtOAc/hexane, 1:2) to give **6e** (17 mg, 0.036 mmol, 13%) as a colorless oil. ^{1}H NMR (400 MHz, $CDCl_3$): δ=3.72 (3H, s), 3.86 (3H, s), 4.14 (2H, s), 6.99 (2H, m), 7.04 (1H, m), 7.30 (1H, m), 7.51 (2H, m), 7.98 (1H, d, J=7.6 Hz), 9.97 ppm (1H, s); ^{13}C NMR (100 MHz, $CDCl_3$): δ=30.4, 52.4, 55.7, 93.1, 102.3, 116.0, 118.7, 128.4, 128.7, 129.6, 129.9, 130.1, 132.7, 140.4, 156.9, 167.8, 170.0, 183.1 ppm; IR (neat): $\tilde{\nu}$=1738, 1686 cm^{-1}. HRMS (ESI) m/z: calcd for $C_{20}H_{16}NO_5I$: 478.0151 [M+H]; 478.0165.

Compound (7), 1-(2-bromo-6-iodobenzoyl)-2-methyl-1*H*-indol: KHMDS (3.0 mL in 0.5 M solution of toluene, 1.5 mmol) was added to a solution of 2-methylindole (100 mg, 0.76 mmol) in THF (2 mL) and stirred at room temperature for 30 min. 2-Bromo-6-iodobenzoyl chloride (751 mg, 2.3 mmol) in THF (2 mL) was added to the mixture at room temperature. After stirring for 2 h at room temperature, the reaction was quenched with H_2O and extracted with AcOEt. The organic layer was washed with saturated aqueous $NaHCO_3$ and dried over Na_2SO_4. After evaporation in vacuo, the residue was purified by silica gel column chromatography (EtOAc/hexane, 1:3) to give **7** (73.2 mg, 0.17 mmol, 22%, *cis*/*trans*, 1:2.0) as a colorless oil. HPLC analysis: eluent = hexane/*i*PrOH, 99:1; Flow rate: 0.5 mL min^{-1}. **7A** [with shorter retention time (27.6 min) in HPLC using CHIRALPAK IB; $[\alpha]_D^{20}$=−32.5 (c=0.2, $CHCl_3$, 96.4% *ee*). **7B** [with a longer retention time (29.9 min) in HPLC using CHIRALPAK IB] $[\alpha]_D^{20}$=+31.7 (c 0.2, $CHCl_3$, 98.5% *ee*). ***cis*-7**: ^{1}H NMR (400 MHz, $CDCl_3$): δ=2.81 (3H, s, CH_3), 6.08 (1H, d, J=8.0 Hz, H7), 6.50 (1H, s, H3), 7.11 (1H, t, J=8.0 Hz), 7.36 (1H, dt, J=1.2, 8.0 Hz, H6), 7.46 (2H, m, H4,H5), 7.69 (1H, dd, J=0.8, 8.0 Hz), 7.91 ppm (1H, dd, J=0.8, 8.0 Hz); ^{13}C NMR (100 MHz, $CDCl_3$): δ=17.4 (*C*H$_3$) {93.1, 110.4, 119.4, 119.8, 120.0, 123.3, 124.4, 130.3, 132.2, 132.9, 135.2, 137.3, 139.5, 142.9}(Ar), 166.6 ppm (N*C*=O). ***trans*-7**: ^{1}H NMR (400 MHz, $CDCl_3$): δ= 1.86 (3H, s, CH_3), 6.40 (1H, s, H3), 7.04 (1H, t, J=8.0 Hz), 7.30 (1H, dd, J=1.2, 7.6 Hz, H6), 7.46 (2H, m, H4, H5), 7.64 (1H, dd, J=1.2, 8.0 Hz), 7.91 (1H, dd, J=1.2, 8.0 Hz), 8.64 ppm (1H, d, J=7.6 Hz, H7); ^{13}C NMR (100 MHz, $CDCl_3$): δ=15.8 (*C*H$_3$), {93.6, 111.8, 112.6, 117.2, 120.0, 123.3, 124.6, 129.8, 132.0, 132.4, 134.7, 138.0, 138.5, 143.2}(Ar), 166.9 ppm (N*C*= O); IR (neat): 1683 cm^{-1}; HRMS (ESI) m/z: calcd for $C_{16}H_{11}NOBrI$: 439.9141 [M+H]; found: 439.9137.

Compound (8), 1-(2-iodo-6-methylbenzoyl)-2-methyl-1*H*-indol: 2-Iodo-6-methylbenzoyl chloride (598 mg, 2.3 mmol) was subjected to treatment with 2-methylindole (100 mg, 0.76 mmol) following the same procedure as that used for the synthesis of **7** described above to afford the product **8** (79.8 mg, 0.21 mmol, 28%, *cis*/*trans*, 1:1.4) as a colorless oil. HPLC: eluent = hexane/*i*PrOH, 99:1. Flow rate: 0.5 mL min^{-1}. **8A** [with shorter retention time (23.3 min) in HPLC using CHIRALPAK IB] $[\alpha]_D^{20}$=−28.6 (c=0.2, $CHCl_3$, 98.8% *ee*). **8B** [with longer retention time (24.8 min) in HPLC using CHIRALPAK IB] $[\alpha]_D^{20}$=+24.6 (c=0.2, $CHCl_3$, 95.8% *ee*). ***cis*-8**: ^{1}H NMR (400 MHz, $CDCl_3$): δ=2.28 (3H, s, CH_3), 2.82 (3H, s, CH_3), 5.96 (1H, d, J=8.4 Hz, H7), 6.49 (1H, s, H3), 6.85 (1H, *t*, J= 8.4 Hz, H6), 7.14 (1H, m), 7.30 (1H, m), 7.45 (2H, m, H4, H5), 7.68 ppm (1H, d, J=8.0); ^{13}C NMR (100 MHz, $CDCl_3$): δ=17.5 (*C*H$_3$), 20.0 (*C*H$_3$), {92.7, 110.1, 112.7, 119.9, 124.2, 129.7 130.3, 130.5, 131.2, 135.5, 136.5, 136.9, 137.2, 142.1}(Ar), 168.7 ppm (N*C*=O). ***trans*-8**: ^{1}H NMR (400 MHz, $CDCl_3$): δ=1.76 (3H, s, CH_3), 2.28 (3H, s, CH_3), 6.38 (1H, s, H3), 7.09 (2H, m), 7.26 (2H, m), 7.30 (1H, m), 7.70 (1H, m), 8.65 ppm (1H, d, J= 8.3 Hz, H7); ^{13}C NMR (100 MHz, $CDCl_3$): δ=15.8 (*C*H$_3$), 20.0 (*C*H$_3$), {93.4, 111.5, 117.3, 119.4, 123.2, 124.5, 130.0, 131.0, 135.1, 136.6, 137.0, 139.4, 142.3}(Ar), 169.1 ppm (N*C*=O); IR (neat): $\tilde{\nu}$=1686 cm^{-1}; HRMS (ESI) m/z calcd for $C_{17}H_{14}NOI$: 376.0193 [M+H]; found: 376.0192;

Compound (9) 1-(2-chloro-6-iodobenzoyl)-2-methyl-1*H*-indol: 2-Chloro-6-iodobenzoyl chloride (644 mg, 2.3 mmol) was treated with 2-methylindole (100 mg, 0.76 mmol) following the same procedure as that used for the synthesis of **7** described above to afford the product **9** (134.4 mg, 0.34 mmol, 45% *cis*/*trans*, 1:1.9) as a colorless oil. HPLC analysis: eluent = hexane/*i*PrOH, 99:1. Flow rate: 0.5 mL min^{-1}. **9A** [with shorter retention time (24.9 min) in HPLC using CHIRALPAK IB] $[\alpha]_D^{20}$=−26.1 (c=0.2, $CHCl_3$, 99.9% *ee*). **9B** [with longer retention time (27.9 min) in HPLC using CHIRALPAK IB] $[\alpha]_D^{20}$=+18.8 (c=0.2, $CHCl_3$, 99.9% *ee*). ***cis*-9**: ^{1}H NMR (400 MHz, $CDCl_3$): δ=2.82 (3H, s, CH_3), 6.08 (1H, d, J= 8.0 Hz, H7), 6.50 (1H, s, H3), 6.90 (1H, t, J=8.0, H6), 7.18 (1H, t, J= 8.0 Hz), 7.34 (1H, dd, J=1.2, 8.0 Hz, H5), 7.52 (2H, m), 7.85 ppm (1H, d, J=8.0 Hz); ^{13}C NMR (100 MHz, $CDCl_3$): δ=17.5 (*C*H$_3$), {93.2, 110.5, 112.5, 119.5, 119.6, 120.8 124.5, 129.9, 130.5, 131.9, 135.3, 137.4, 139.5, 141.3}(Ar), 165.9 ppm (N*C*=O). ***trans*-9**: ^{1}H NMR (400 MHz, $CDCl_3$): δ= 1.85 (3H, s, CH_3), 6.38 (1H, s, H3), 7.11 (1H, t, J=8.0 Hz), 7.28 (1H, dd, J=1.2, 8.0 Hz), 7.52 (3H, m, H4, H6, Ar), 7.81 (1H, d, J=8.0 Hz), 8.64 ppm (1H, d, J=8.0 Hz, H7); ^{13}C NMR (100 MHz, $CDCl_3$): δ=15.7 (*C*H$_3$), {93.8, 111.9, 117.2, 119.6, 120.2, 123.4, 124.7, 129.5, 131.7, 132.1, 137.7, 138.1, 137.7, 141.6}(Ar), 166.2 ppm (N*C*=O); IR (neat): $\tilde{\nu}$= 1686 cm^{-1}; HRMS (ESI) m/z calcd for $C_{16}H_{11}NOClI$: 395.9647 [M+H]; found: 395.9652.

Single-crystal X-ray analysis: Single-crystal X-ray diffraction data of the crystals were collected on a CCD diffractometer with graphite monochromated $Mo_{K\alpha}$ radiation. The data were collected at low temperature (90 K) by using liquid nitrogen. The structure was solved by the direct method SHELXS-97[15] and refined by full-matrix least-squares SHELXL-97. The non-hydrogen atoms were refined anisotropically.

Crystal Data for 5e: $C_{20}H_{18}O_4NBr$, M_r=416.26, $Mo_{K\alpha}$ (λ=0.71073 Å), monoclinic, *C2/c*, colorless prism 0.10×0.05×0.05 mm, crystal dimensions a=21.2964 (17) Å, b=8.2148(7) Å, c=21.8966 (18) Å, α=90°, β= 108.5550(10)°, γ=90°, T=90 K, Z=8, V=3631.6 (5) Å^3, D_{calcd}= 1.523 g cm^{-3}, F_{000}=1696, GOF=1.021, R_{int}=0.0324, R_1=0.0346, wR_2= 0.0791. CCDC-918030 (**5e**) contain the supplementary crystallographic data for this paper. These data can be obtained free of charge from The Cambridge Crystallographic Data Centre via www.ccdc.cam.ac.uk/data_request/cif.

Acknowledgements

This work was supported in part by a Grant-in-Aid for Scientific Research (C) (21590124) and a Grant-in-Aid for Young Scientists (B) (21790025) from the Japan Society for the Promotion of Science.

[1] a) A. M. Fulton, *Cancer Res.* **1984**, *44*, 2416–2420; b) D. Hwang, D. Scollard, J. Byrne, E. Levine, *J. Natl. Cancer Inst.* **1998**, *90*, 455–456.

[2] a) K. R. Gans, W. Galbraith, R. J. Roman, S. B. Haber, J. S. Kerr, W. K. Schmidt, C. Smith, W. E. Hewes, N. R. Ackerman, *J. Pharmacol. Exp. Ther.* **1990**, *254*, 180–187; b) T. D. Penning, J. J. Talley, S. R. Bertenshaw, J. S. Carter, P. W. Collins, S. Docter, M. J. Graneto, L. F. Lee, J. W. Malecha, J. M. Miyashiro, R. S. Rogers, D. J. Rogier, S. S. Yu, G. D. Anderson, E. G. Burton, J. N. Cogburn, S. A. Gregory, C. M. Koboldt, W. E. Perkins, K. Seibert, A. W. Veenhuizen, Y. Y. Zhang, P. C. Isakson, *J. Med. Chem.* **1997**, *40*, 1347–1365; c) A. S. Kalgutkar, A. B. Marnett, B. C. Crews, R. P. Remmel, L. J. Marnett, *J. Med. Chem.* **2000**, *43*, 2860–2870; d) A. S. Kalgutkar, B. C. Crews, S. W. Rowlinson, A. B. Marnett, K. R. Kozak, R. P. Remmel, L. J. P. Marnett, *Proc. Natl. Acad. Sci. USA* **2000**, *97*, 925–930.

[3] P. J. Loll, D. Picot, O. Ekabo, R. M. Gravito, *Biochemistry* **1996**, *35*, 7330–7340.

[4] R. G. Kurumbail, A. M. Stevens, J. K. Gierse, J. J. McDonald, R. A. Stegeman, J. Y. Pak, D. Gildehaus, J. M. Miyashiro, T. D. Penning, K. Seibert, P. C. Isakson, W. C. Stallings, *Nature* **1996**, *384*, 644–648.

[5] a) H. Kakuta, X. Zheng, H. Oda, S. Harada, Y. Sugimoto, K. Sasaki, A. Tai, *J. Med. Chem.* **2008**, *51*, 2400–2411; b) Y. Kasaya, K. Hoshi, Y. Terada, A. Nishida, S. Shuto, M. Arisawa, *Eur. J. Org. Chem.* **2009**, 4606–4613; c) M. Arisawa, Y. Kasaya, T. Obata, T. Sasaki, M. Ito, H. Abe, Y. Ito, A. Yamano, S. Shuto, *ACS Med. Chem. Lett.* **2011**, *2*, 353–357; d) M. Arisawa, Y. Kasaya, T. Obata, T. Sasaki, T. Nakamura, T. Araki, K. Yamamoto, A. Sasaki, A. Yamano, M. Ito, H. Abe, Y. Ito, S. Shuto, *J. Med. Chem.* **2012**, *55*, 8152–8163.

[6] a) P. J. Loll, R. M. Gravito, C. J. Carrell, H. L. Carrell, *Acta Crystallogr. Sect. C* **1996**, *52*, 455–457; b) X. Chen, K. R. Morris, U. J. Griesser, S. R. Byrn, J. G. Stowell, *J. Am. Chem. Soc.* **2002**, *124*, 15012–15019.

[7] H. Takahashi, S. Wakamatsu, H. Tabata, T. Oshitari, A. Harada, K. Inoue, H. Natsugari, *Org. Lett.* **2011**, *13*, 760–763.

[8] A. R. Katritzky, L. Khelashvili, P. P. Mohapatra, P. J. Steel, *Synthesis* **2007**, 3673–3677.

[9] See the Supporting Information for the synthesis of **3**.

[10] See the Supporting Information for the synthesis of **4a** and **5a–e**.

[11] We recognize that the one set of resonances can be the averaged conformers of compounds **4–6**.

[12] See the Supporting Information for the NOE correlation of **5e** (*trans*-like), and the NOESY spectrum of **6d** (*cis*-like).

[13] M. Petit, A. J. B. Lapierre, D. P. Curran, *J. Am. Chem. Soc.* **2005**, *127*, 14994–14995.

[14] The IC_{50} values for COX-1 are almost same as for the racemate **1** and the active enantiomer (−)-**1**, as shown in Table 2, although theoretically the former should be two-fold the value of the latter. Although this phenomenon cannot be clearly explained at present, the relatively weak IC_{50} values (on the order of 10 μM) may make it difficult to differentiate clearly the potencies of **1** and (−)-**1**.

[15] A short history of SHELX: G. M. Sheldrick, *Acta Crystallogr. A* **2008**, *64*, 112–122.

Received: January 8, 2013
Published online: April 9, 2013

